Soft Matter

PAPER

View Article Online
View Journal | View Issue

Cite this: *Soft Matter*, 2024, **20**, 5745

Structural determinants of collapse by a monomolecular mimic of pulmonary surfactant at the physiological temperature†

Fazle R. Dayeen,‡[a] Bret A. Brandner,‡[b] Wei Bu,[c] Stephen B. Hall *[b] and David Gidalevitz *[a]

Pulmonary surfactant forms a thin film on the liquid that lines the alveolar air-sacks. When compressed by the decreasing alveolar surface area during exhalation, the films avoid collapse from the air/water interface and reduce surface tension to exceptionally low levels. To define better the structure of compressed films that determines their susceptibility to collapse, we measured how cholesterol affects the structure and collapse of dipalmitoyl phosphatidylcholine (DPPC) monolayers at physiological temperatures. Grazing incidence X-ray diffraction (GIXD) and grazing incidence X-ray off-specular scattering (GIXOS) established the lateral and transverse structures of films on a Langmuir trough at a surface pressure of 45 mN m^{-1}, just below the equilibrium spreading pressure at which collapse begins. Experiments with captive bubbles at a surface pressure of 51 mN m^{-1} measured how the steroid affects isobaric collapse. Mol fractions of the steroid (X_{chol}) at 0.05 removed the tilt by the acyl chains of DPPC, shifted the unit cell from centered rectangular to hexagonal, and dramatically decreased the long-range order. Higher X_{chol} produced no further change in diffraction, suggesting that cholesterol partitions into a coexisting disordered phase. Cholesterol had minimal effect on rates of collapse until X_{chol} reached 0.20. Our results demonstrate that the decreased coherence length, indicating conversion of positional order to short-range, is insufficient to make a condensed monolayer susceptible to collapse. Our findings suggest a two-step process by which cholesterol induces disorder. The steroid would first convert the film with crystalline chains to a hexatic phase before generating a fully disordered structure that is susceptible to collapse. These results lead to far-reaching consequences for formulation of animal-derived therapeutic surfactants. Our results suggest that removal of cholesterol from these preparations should be unnecessary below X_{chol} = 0.20.

Received 23rd April 2024,
Accepted 30th June 2024

DOI: 10.1039/d4sm00481g

rsc.li/soft-matter-journal

Introduction

The studies reported here address the structural determinants of the susceptibility to collapse by phospholipid monolayers. When compressed at an air/water interface under equilibrium conditions, fluid monolayers undergo a phase transition at the equilibrium spreading tension.[1] Constituents of the two-dimensional films collapse from the interface to form their three-dimensional bulk phase. Further compression fails to increase the interfacial density of the monolayer, and surface tension at equilibrium falls no further. Collapse of the films limits access to surface tensions below the equilibrium spreading value, which for phospholipids is ~25 mN m^{-1}.

Collapse has important consequences, including physiological. Pulmonary surfactant is the mixture of lipids and proteins secreted by the lungs that lowers surface tension in the alveolar air-sacks. The mixture adsorbs to the surface of the liquid that lines the alveoli and forms a thin film.[2] When compressed by the decreasing alveolar surface area during exhalation, the films avoid collapse. They reduce surface tension to exceptionally low values, ~1–2 mN m^{-1}.[3–10] Low surface tensions are essential for alveolar integrity during normal breathing. In lungs that lack adequate amounts of pulmonary surfactant, elevated surface tensions tend to deflate the alveoli. The stresses involved in repeatedly reopening deflated air-spaces[11,12] progressively damage the thin barrier that separates alveolar air from capillary blood.[13,14]

[a] *Department of Physics, Center for Molecular Study of Condensed Soft Matter (μCoSM), Illinois Institute of Technology, Chicago, IL 60616, USA. E-mail: gidalevitz@iit.edu*
[b] *Pulmonary & Critical Care Medicine, Oregon Health & Science University (OHSU), Portland, OR 97239-3098, USA. E-mail: sbh@ohsu.edu*
[c] *NSF's ChemMatCARS, Pritzker School of Molecular Engineering, University of Chicago, Chicago, Illinois 60637, USA*

† Electronic supplementary information (ESI) available. See DOI: https://doi.org/10.1039/d4sm00481g

‡ Equal contributors.

The structure of phospholipid monolayers determines their susceptibility to collapse. Appropriate compounds can form condensed films in which their acyl chains occupy a crystalline lattice.[15] When compressed, those films avoid collapse. At temperatures below its main transition temperature, for instance, monolayers of dipalmitoyl phosphatidylcholine (DPPC) form a two-dimensional centered-rectangular structure that resists collapse.[16] The films readily undergo compression to very low surface tensions. Above the melting temperature,[17,18] disordered films of that compound collapse at the equilibrium spreading tension. DPPC is the only major component of pulmonary surfactant that, by itself at physiological temperatures, forms Lβ or Lβ, bilayers. Each leaflet in these bilayers has the same crystalline structure as a condensed monolayer, distinguished from each other only by tilt of the acyl chains in the Lβ, phase. The most widely held model of how pulmonary surfactant achieves low surface tensions contends that the alveolar film has the structure of condensed DPPC.[19]

In addition to phospholipids and proteins, pulmonary surfactant contains cholesterol. In sufficient amounts, that compound makes films of pulmonary surfactant susceptible to collapse.[20–22] The steroid also promotes collapse of DPPC monolayers[16,23] and alters their structure.[16] At ambient laboratory temperatures, the dose–response of the changes in structure and rates of collapse are discordant.[16] Doses of cholesterol that first change the structure of the DPPC monolayer are well below the levels at which collapse abruptly accelerates.

This observation suggests that cholesterol induces disorder in two steps. The process would be analogous to the melting of strictly two-dimensional crystals.[24] Heating those structures first forms a hexatic phase, in which positional order changes from quasi long-range to short-range. The hexatic structure, however, retains bond-orientational order, defined by quasi-long-range order in the orientation among neighboring constituents. Further heating disrupts orientational order, resulting in a disordered structure. The experiments here, conducted at physiological temperatures, used X-ray scattering to determine the structural changes in DPPC monolayers produced by cholesterol. Our studies establish the correlation between the structure and function of DPPC-monolayers in response to increasing amounts of cholesterol at the conditions where collapse begins.

Materials and methods

Materials

The following items were purchased commercially, and used as received: DPPC, Avanti Polar Lipids (Alabaster, AL); cholesterol (purity > 99%), Sigma-Aldrich (St. Louis, MO); HPLC-grade chloroform (EMD Millipore, Burlington, MA); *N*-2-hydroxyethylpiperazine-*N*′-2-ethane sulfonic acid (Hepes) (Sigma, St. Louis, MO); $CaCl_2{\cdot}2H_2O$ and NaCl (Mallinckrodt, Hazelwood, MO). The composition of the mixed lipids was expressed as the mol fraction of the steroid (X_{chol}). Water processed either by a barnstead nanopure diamond purification system (Dubuque, IA) at OHSU or with a MilliporeSigma Milli Q system (Burlington, MA) at the Advanced Photon Source (APS, Argonne National Laboratory, Argonne, IL) yielded a resistance ≥ 18.2 MΩ. Buffered electrolyte contained 10 mM Hepes pH 7.0, 150 mM NaCl, 1.5 mM $CaCl_2$ (HSC).

Methods

Surface X-ray scattering. Our studies used X-ray scattering to determine how cholesterol altered the structure of DPPC monolayers. The films were spread on a subphase of HSC in a Langmuir trough at Sector 15-ID-C of the APS. A sealed enclosure allowed replacement of the ambient atmosphere with helium to minimize background scattering. All measured intensities were normalized relative to the intensity of the incident beam.

Evaporation of the subphase has complicated measurements of X-ray scattering from monolayers on a liquid subphase at temperatures above ambient levels. Shifts in the vertical location of the interface can produce drastic changes in the scattered intensity at the detector. Condensation on the windows into the enclosing chamber can also decrease the detected intensity, as well as increase background scattering. These problems have constrained almost all prior measurements of X-ray scattering from the air/water interface to ambient or lower temperatures.

The experiments here, conducted at physiological temperatures, used heaters installed on the Kapton windows to eliminate the problem of condensation. Scans conducted every 20 minutes monitored the height of the interface. Buffer added to the subphase maintained the monolayer at a constant level.

Deposition of chloroform solutions at ambient temperatures formed films at surface pressures < 45 mN m^{-1}. After evaporation of the spreading solvent, heating the trough and environment increased temperature to 37 °C. Compression of the film then elevated surface pressure to 45 mN m^{-1}, which was maintained for the duration of the measurements.

Grazing incidence X-ray diffraction (GIXD). Scattering of an X-ray beam incident on the air/water interface at a grazing angle provides the in-plane, lateral structure of a film. For a beam incident below the critical angle, the diffracted intensity is a function of the momentum transfer parallel to the surface, q_{xy}, given by

$$q_{xy} = \frac{4\pi}{\lambda}\sin\left(\frac{2\theta}{2}\right)$$

for an angle of 2θ between the incident and diffracted beams. The measurements of GIXD here used an X-ray beam with a wavelength, λ, of 1.24 Å incident at 85% of the critical angle (q_c = 0.0217 $Å^{-1}$). All measured intensities were normalized relative to the intensity of the incident beam, measured at the beam-stop.

Integration of the diffracted intensity over q_z provided the variation of scattering with q_{xy}. After subtracting background, the program OriginPro (Northampton, MA) provided the best fit of the data to one or two Lorentz–Gauss (1 : 1) crossed peaks. Based on the relative quality of the fit, analysis of the traces

used two peaks for the samples at X_{chol} = 0.00 and 0.05, but one peak for the remaining compositions. The q_{xy} of a fitted peak yielded the repeat distances between the diffracting hydrocarbon chains,

$$d_{h,k} = \frac{2\pi}{q_{xy}}$$

for the Miller indices, h and k. The breadth of the peak provided the coherence length, L_{xy}, of the diffracting region according to the Sherrer formula,[25]

$$L_{xy} = 0.9\frac{2\pi}{\xi_{h,k}}$$

where $\xi = (\mathrm{FWHM}^2 - \Delta^2)^{1/2}$ for the full width of the peak at the half-maximum (FWHM), with instrumental resolution (Δ) of 9.56 × 10^{-3} Å^{-1}.

For diffraction with two-peaks, the molecular tilt, τ, of chains toward their nearest neighbor is determined by[26]

$$d_{11} = \frac{d_{02}}{\left[\left(\frac{d_{02}^4}{A_0^2}\right)\cos^2\tau + \frac{1}{4}\right]^{\frac{1}{2}}}$$

where the lattice spacings d_{11} and d_{02} correspond to planes with Miller indices of {1 1,1 −1} and {0 2}, and A_0 is the area of the unit cell.[27]

Grazing incidence X-ray off-specular scattering (GIXOS). To obtain the electron-density profile of the films perpendicular to the interface, our studies used GIXOS[28,29] rather than the more common X-ray reflectivity (XR). Instead of the approach used by XR of measuring the reflected beam in the specular plane, GIXOS analyses diffuse off-specular scattering generated by capillary waves. Measurements used a fixed geometry to collect the scattering pattern. The X-ray beam was incident on the surface at an angle of α = 0.1°, just below the critical angle. The azimuthal angle, 2θ, was set at 0.3°. A two-dimensional hybrid pixel-array detector (PILATUS3 200K) (Dectris, Baden-Dättwil, Switzerland) measured intensities in a single-photon counting mode over the range of horizontal angles, β, from the specular plane between 0.0 and 7.3°. The drastic decrease in intensity with increasing q_z, which is ubiquitous for specular reflectivity, is meagre in the diffuse scattering signal. This effect provides a significant advantage for GIXOS over XR. The time required to collect data is significantly reduced. Rather than measuring the intensities at a series of β values, the experiment requires only two exposures – one for the sample, and a second for the background.

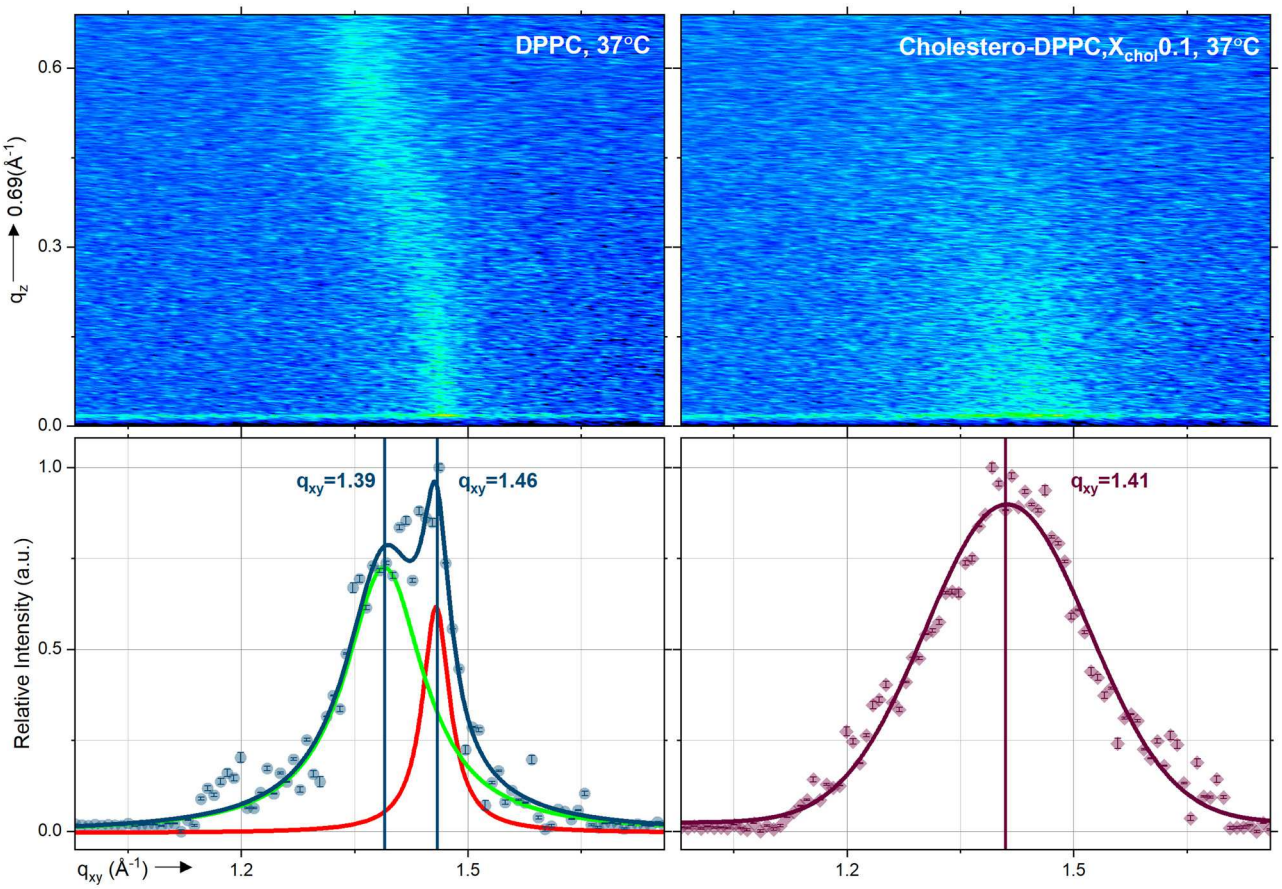

Fig. 1 GIXD from monolayers of DPPC without and with (X_{chol} = 0.10) cholesterol. Measurements were made at a surface pressure of 45 mN m^{-1}, just below the equilibrium spreading pressure of 46.5 mN m^{-1}, and physiological temperature of 37 °C. Panels in the upper row give the imaged intensities. The lower row provides the variation of intensities integrated over q_z. Continuous curves represent the best fits to the data using Lorentz–Gauss crossed peaks. Errors are assumed to be Poisson-distributed.

Relative to XR, GIXOS requires experiments of much shorter duration, which greatly simplifies measurements at elevated temperatures. Evaporation and shifts of the interfacial location during the experiments at 37 °C were insignificant.

GIXOS offers additional advantages over XR. The measurements use an incident beam at a grazing angle. The footprint of the beam is consequently larger than with XR. Measurements that sample a larger area are less sensitive to lateral inhomogeneities in the film. The incident radiation is also less likely to damage the film.[29]

Simulations of the measured GIXOS used a model-dependent approach based on Parratt's multilayer recursive formalism.[30] By allowing the interfacial roughness and the electron density of the headgroups and hydrocarbon tails to vary during the fitting, a least-squares algorithm minimized the deviation between the experimental data and calculated profile.

Collapse. We measured the kinetics of collapse by films held at constant surface pressure. To the extent that any surface pressure corresponds to a unique interfacial concentration, isobaric changes in area are proportional to molecular adsorption or desorption.[31] Collapse of fluid phospholipids begins at the equilibrium spreading pressure of ~46 mN m^{-1}. Rates of collapse by fluid films at higher surface pressures vary anomalously, reaching a maximum value at 52 mN m^{-1} and then declining.[32] Our experiments measured isobaric collapse at a surface pressure of 51 mN m^{-1}. Aliquots of solutions in chloroform deposited on the surface of captive bubbles in a subphase of HSC formed monomolecular films. Exhaustive exchange of the subphase removed the spreading solvent.[17] Heating pads applied to the sides of the chamber[17,33] containing the bubble increased temperature to 37 °C. Analysis of the bubble's profile viewed along the horizontal axis[34] determined surface area and surface pressure.[35,36] Two cycles of slow expansion and compression at surface pressures below 45 mN m^{-1} served to anneal the film.[16] A pulsed compression then raised surface pressure to the target value, which was held constant using simple feedback (ESI†).[32] The initial slope of semilogarithmic plots of area *versus* time provided the rate of collapse.

Results

GIXD

Even the lowest level of added cholesterol, at X_{chol} = 0.05, altered the structure of the DPPC monolayer. DPPC by itself produced two peaks of diffraction similar to results at ambient temperatures (Fig. 1 (left panels) and 2).[16] The two peaks indicated a centered-rectangular unit cell. Off-equatorial scattering, at $q_z > 0$, indicated tilt of the acyl chains (Table 1). Cholesterol at X_{chol} = 0.05 centered the scattered intensity at q_z = 0, establishing the absence of tilt (Fig. 1 (right panels) and 2). A single Bragg peak dominated the lateral distribution of scattered intensity (Fig. 2), with a minimal contribution by the {0 2} peak of the centered-rectangular lattice ubiquitous for DPPC without cholesterol. The shift indicated the transition from a centered-rectangular unit cell to a structure dominated by a hexagonal lattice, in which the distances between all scattering neighbors are equal.[37] These changes at 37 °C were similar to the effects of cholesterol at 23 °C, although at a lower X_{chol} (0.05 rather than 0.10).

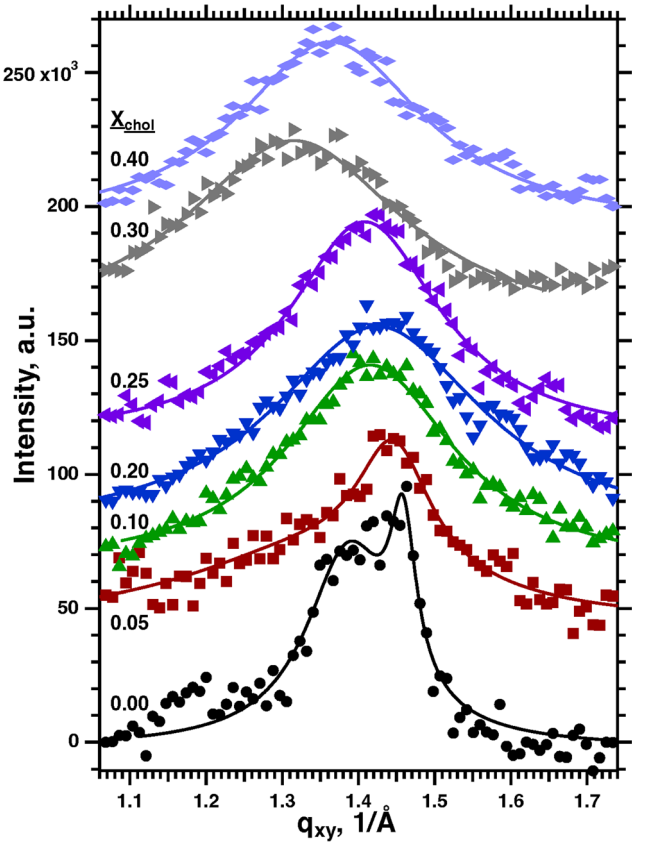

Fig. 2 Grazing incidence X-ray diffraction (GIXD) from spread monolayers of DPPC with different mol fractions of cholesterol (X_{chol}) at 37 °C. The scattering vector, q_{xy}, expresses the angular dependence according to $q_{xy} = 4\pi \sin\theta/\lambda$, where λ is the wavelength of the incident beam, and the angle between the incident and scattered beams is 2θ. Symbols give measured intensities in arbitrary units (a.u.). Continuous curves give the least-squares fit to the experimental data by the sum of two Lorentzians for films with X_{chol} of 0.00 and 0.05, and by a single Lorentzian for films with more cholesterol. The points and curves are shifted vertically without change in scale for clarity of presentation.

Table 1 Lateral structure of the ordered phase in DPPC/cholesterol films at 37 °C

X_{chol}	*d*-spacing (Å ± 0.01)	L_{xy} (Å)	*a*, *b*^{a} (Å ± 0.1)	A_{UC}^{b} (Å^2 ± 0.1)	τ (deg.)
0.00	$d_{(1,1),(1,-1)}$ = 4.52	43.0	5.22	44.9	29.9
	$d_{(0,2)}$ = 4.30	139	8.61		
0.05	$d_{(1,1),(1,-1)}$ = 4.62	11.0	5.33	46.5	0
	$d_{(0,2)}$ = 4.36	54.0	8.72		
0.10	4.46	21.4	5.15	45.9	0
0.20	4.42	17.3	5.11	45.2	0
0.25	4.46	22.4	5.15	45.9	0
0.30	4.80	16.1	5.54	53.1	0
0.40	4.62	18.7	5.33	49.3	0

A_{UC} – area per unit cell; τ - angle of molecular tilt from the surface normal. ^{a} For a centered rectangular unit cell, dimensions $a \neq b$. For a hexagonal unit cell, $a = b$. ^{b} A_{UC} contains two alkyl chains.

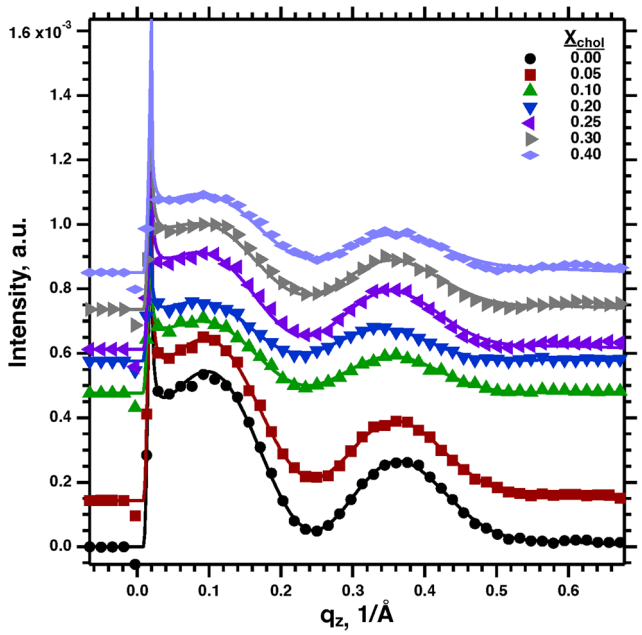

Fig. 3 Diffuse scattering obtained by GIXOS. Symbols give measured intensities for films with different X_{chol}. Continuous curves represent the best fit of a model of the interface as sequential slabs of uniform thickness. Data are shifted vertically without change in scale for clarity of presentation.

Cholesterol also broadened the distribution of the scattered intensity (Fig. 2). According to the Scherrer formula,[25] the breadth of the GIXD peak is inversely proportional to the coherence length, L_{xy}, of the ordered domains (Table 1). L_{xy} at 37 °C fell to values below 2 nm. In addition to altering the structure of the monolayer, even small amounts of cholesterol induced significantly smaller ordered domains.

Increasing cholesterol above X_{chol} = 0.05 produced minimal change in the hexagonal structure. The scattered intensity continued to fit within a single peak (Fig. 2) centered on the equator, indicating hexagonal symmetry with untilted chains. The q_{xy} of the diffraction peak was unchanged (Fig. 2), demonstrating that despite the added steroid, the lattice constant remained fixed (Table 1). The coherence length changed minimally (Table 1). Once formed, the structure of the hexagonal phase was essentially invariant to the addition of more cholesterol.

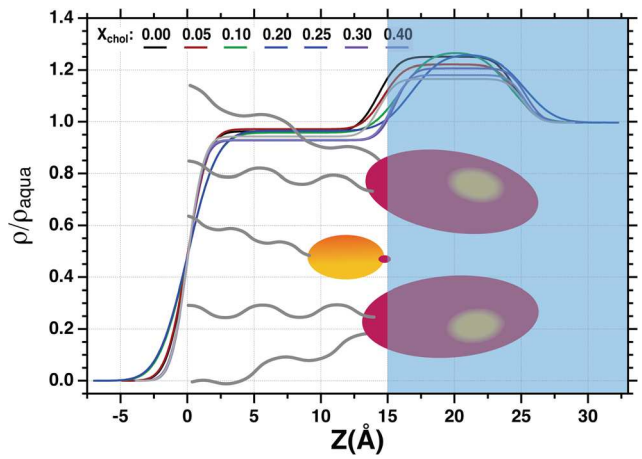

Fig. 4 Electron density profiles for films with different X_{chol} at 37 °C obtained by GIXOS. Electron density (ρ) is normalized relative to the value for water (ρ_{aqua}). Z gives the distance from the top of the upper layer, defined by the mid-point of the rise in the normalized density from the value for air to the first plateau. The curves give the best fit of a two-slab model to the experimental data. The blue slab and molecular cartoons indicate the locations of the aqueous subphase and the air/water interface, as well as the components of the film. The footprint of the incident, grazing beam is sufficiently large that the results should represent the average effects of the coexisting phases.

GIXOS

In addition to the lateral structure of the film, X-ray scattering can determine the distribution of the electron density across the air–water interface. Measurements of X-ray reflectivity (XR) in the specular plane commonly provide that information. Those experiments, however, require prolonged exposures that complicate experiments above ambient temperatures. The studies here therefore used the more recently developed grazing-incident X-ray off-specular scattering (GIXOS), which avoids that problem.[28]

Progressively larger amounts of cholesterol added to the DPPC produced minimal changes in the X-ray scattering obtained by GIXOS (Fig. 3). Those changes showed no consistent dose-related response beyond X_{chol} = 0.05. The differences were insufficient to alter the electron density profiles significantly (Fig. 4). The electron density profiles within the monolayers were also very similar. The plateau of constant electron density adjacent to the interface had similar values and extent at different X_{chol} (Fig. 4). The region with higher density, corresponding to the phospholipid headgroup, was unaffected. The thickness of the films remained essentially constant, and monomolecular. Cholesterol had no meaningful effect on the structure of the films perpendicular to the interface.

Collapse

Cholesterol above a threshold value produced a dramatic change in the rates at which the films collapsed (Fig. 5). Up to X_{chol} = 0.20, incremental increases in cholesterol produced collapse that was minimally faster. Between X_{chol} = 0.20 and 0.30, the rate of collapse increased relative to the initial change at lower X_{chol} by an order of magnitude. At X_{chol} = 0.40, the rate of collapse exceeded our ability to maintain isobaric conditions. The rates at 37 °C were faster than the previously determined collapse at 23 °C,[16] but the dependence on X_{chol} was remarkably similar (Fig. 5).

Discussion

Our results suggest that at the physiological temperature, cholesterol induces monolayers of DPPC to undergo structural changes in two stages. Only the second step would make the films susceptible to collapse.

The changes produced by cholesterol are similar at 23 and 37 °C. Small amounts of the steroid eliminate tilt of the acyl chains, and shift the centered rectangular unit cell for DPPC

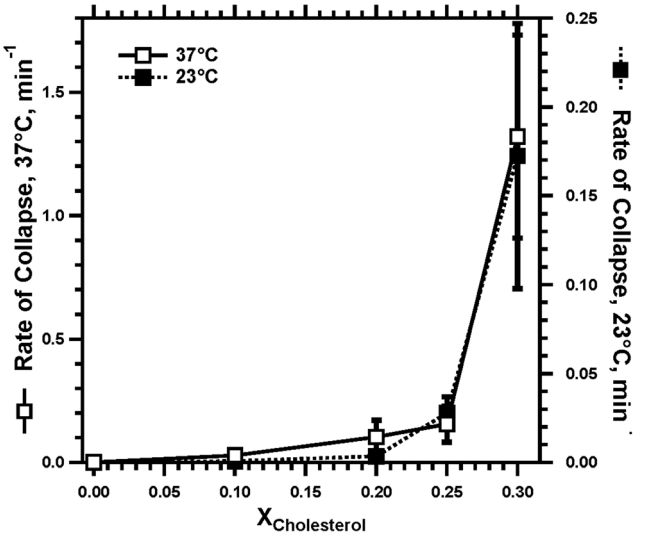

Fig. 5 Dependence of isobaric collapse by monomolecular films of DPPC on content of cholesterol. Films were held at surface pressure = 51 mN m^{-1} during collapse. Rates were determined from the initial slope of linear fits to semilogarithmic plots of area *versus* time. Left axis gives rates measured here at 37 °C (solid line, open squares). Right axis gives rates measured previously,[16] determined at 23 °C (dotted line, filled squares). Mean ± S.D.

alone to hexagonal symmetry, although at a lower level of cholesterol for the higher temperature (X_{chol} = 0.05) than at 23 °C (X_{chol} = 0.10). Rates of collapse are faster, as expected, at the higher temperature, but the qualitative behavior is the same. Cholesterol has relatively little effect below X_{chol} = 0.20, but the rate of collapse increases rapidly at higher levels.

Cholesterol also increases the GIXD peak-width at both temperatures. This result indicates that the coherence length, L_{xy}, and the size of the crystalline domains decreases. The effect at 37 °C is dramatic. The broader diffraction peak indicates that the size of coherent ordered domains falls to 3–4 intermolecular distances. At the physiological temperature, low levels of cholesterol convert positional order in the DPPC films from long- to short-range.

Despite the loss of long-range positional order, that structure remains resistant to collapse. Cholesterol above X_{chol} = 0.05 produces no further change in the ordered structure. The acyl chains of the phospholipid remain untilted. The unit cell remains hexagonal with the same lattice constant up to X_{chol} = 0.25. Further increase of the cholesterol content up to X_{chol} = 0.4 results in no increase of the hexagonal lattice parameter. The coherence length varies minimally without a consistent trend. The electron density profile normal to the interface is unchanged throughout the entire range of the cholesterol concentrations used. The structure of the hexagonal phase is the same below and above the X_{chol} at which rates of collapse increase dramatically. The hexagonal phase is not the structure that is susceptible to collapse.

The invariance of the hexagonal structure to added cholesterol at X_{chol} = 0.05 to 0.25 suggests the nature of the structure that does collapse. Partitioning of the steroid into a disordered coexisting phase would explain the absence of an evident structural effect. The Gibbs phase rule would require that the chemical potential, and composition, of each coexisting phase would remain constant.[38] A system with two components, two phases, and no unfixed intensive variable would have no degrees of freedom. Added cholesterol would convert the hexagonal phase to the coexisting structure and enlarge its area. The stoichiometry, and local structure, of each phase would remain the same.

The lack of any change in GIXD with added cholesterol indicates that any new induced structure must be disordered. Such a structure would generate no diffraction, and be undetectable by GIXD. A disordered structure should be fluid, and susceptible to collapse. Growth of the disordered phase would at some point achieve a level sufficient to allow collapse of the film.

Our data suggest that the hexagonal structure induced by low levels of cholesterol is a hexatic phase. Our films include characteristics of hexatic structures,[37] such as six-fold symmetry. The width of the diffraction peak exceeds the limit of instrumental resolution, indicating that the ordered structure is not a two-dimensional crystal. The GIXD lacks the intensity in the wings of the peak that would indicate a two-dimensional liquid. Along with short-range positional order, these properties fit with a hexatic phase.

A key feature of the hexatic phase is the presence of quasi-long-range bond-orientational order, defined by the orientation among neighboring constituents. Because the chains, at least on average, are perpendicular to the interface, GIXD provides no information on orientation.[39] Results with cholesterol-DPPC at other conditions nonetheless suggest that during the initial structural change, preservation of long-range orientational order is likely. In monolayers with tilted chains, tilt is greater at lower surface pressures. At ambient temperatures and lower surface pressures, the chains of DPPC remain tilted with low levels of cholesterol.[40] Long-range orientational order persists. Extension of this result to conditions that eliminate tilt would indicate that the initial structure induced by cholesterol here is most likely a hexatic phase.

The behavior induced by cholesterol would then be analogous to the melting of two-dimensional crystals,[24,41,42] and to the disorder/order transitions in compressed Langmuir monolayers.[40,41,43] Higher temperatures and lower surface pressures initially convert those ordered systems to a hexatic phase, in which positional order becomes short-range.[44,45] Bond-orientational order remains quasi long-range. The second step in melting or expansion is the conversion of orientational order to short-range. That change yields a disordered structure.

That sequence of structural shifts would explain the functional alterations. The onset of rapid collapse would require growth of the disordered phase. Like the melting of hexatic films, that second disordering step would involve the loss of long-range orientational order. Although this scheme is appealing, our evidence for that orientational change is indirect. The most certain conclusion from our results is that the loss of long-range positional order by itself is insufficient to induce susceptibility to collapse.

Our studies use DPPC-cholesterol monolayers with varying X_{chol} as models of the functional alveolar film. This approach is

based on prior studies with the complete set of surfactant lipids. Fluorescence microscopy shows that monolayers containing only the full complement of surfactant phospholipids form coexisting phases.[46] Compositional analysis performed upon films with increasing DPPC contents indicates that the mixture behaves as a pseudobinary system where the more ordered phase contains only DPPC.[46] All of the other phospholipids partition into the surrounding, disordered film along with a fraction of DPPC. Additionally, measurements of surface potential suggest that physiological levels of cholesterol partition into the ordered domains.[47] A widely considered view contends that the functional alveolar film forms during compression by differential exclusion of the coexisting phases. The effect of cholesterol on pure DPPC in our studies here is directly relevant to the behavior of films containing the complete mixture of surfactant constituents.

Our results have important biomedical implications. Neonates lack adequate amounts of endogenous surfactant if born prior to ~32 weeks of gestation. Normal breathing with increased alveolar surface tensons injures the alveolocapillary barrier. The babies develop the pulmonary edema and hypoxia of the respiratory distress syndrome (RDS).[13] Exogenous therapeutic surfactants have greatly improved the survival of babies at risk for RDS.[48] Therapeutic surfactants from animals have proven superior to artificial preparations.[49] Cholesterol is removed from almost all animal-derived agents because of the evidence that sufficient amounts of the steroid induce faster collapse. The process of removing cholesterol can also essentially eliminate essential elements of pulmonary surfactant, such as the hydrophobic surfactant protein, SP-B.[50] For calf surfactant, the mol fraction of cholesterol used here of X_{chol} = chol/(chol + DPPC) is 0.20. Our results suggest that removal of cholesterol from the animal-derived surfactant preparations should be unnecessary, and possibly counterproductive.

Conclusions

Cholesterol causes DPPC monolayers to undergo changes in structure and susceptibility to collapse at different X_{chol}. That behavior raises the possibility that the steroid increases disorder in two steps. GIXD indicates that cholesterol initially induces the loss of long-range positional order without affecting collapse. Our results suggest that additional cholesterol induces a second step in which DPPC forms a fully disordered phase that is capable of collapse. Extension of results at lower surface pressures with less cholesterol, where the presence of tilt allows evaluation of orientation among adjacent chains, suggests that the initial structure which resists collapse is hexatic. Our results demonstrate that long-range positional order is unnecessary for the alveolar film to avoid collapse and sustain very low surface tensions.

Author contributions

Fazle Dayeen performed X-ray scattering experiments and analyzed the results. Bret Brandner prepared the samples, measured rates of collapse, and analyzed the results. Stephen Hall designed the studies, analyzed the measurements of collapse, and wrote the manuscript. David Gidalevitz designed the studies, performed X-ray scattering experiments, analyzed the results, and wrote the manuscript.

Data availability

The data that support the findings of this study are available from the corresponding authors upon reasonable request.

Conflicts of interest

None.

Acknowledgements

Funds from the National Institutes of Health (HL130130 and 136734) supported this research. ChemMatCARS Sector 15 is supported by the National Science Foundation under grant number NSF/CHE-1834750. This research used resources of the Advanced Photon Source, a U.S. Department of Energy (DOE) Office of Science User Facility operated for the DOE Office of Science by Argonne National Laboratory under Contract No. DE-AC02-06CH11357.

References

1 G. L. Gaines Jr., *Insoluble Monolayers at Liquid-Gas Interfaces*, Interscience Publishers, New York, 1966; p. 147.
2 J. Bastacky, C. Y. Lee, J. Goerke, H. Koushafar, D. Yager, L. Kenaga, T. P. Speed, Y. Chen and J. A. Clements, Alveolar lining layer is thin and continuous: low-temperature scanning electron microscopy of rat lung, *J. Appl. Physiol.*, 1995, **79**, 1615–1628.
3 H. Bachofen, J. Hildebrandt and M. Bachofen, Pressure-volume curves of air- and liquid-filled excised lungs-surface tension in situ, *J. Appl. Physiol.*, 1970, **29**, 422–431.
4 T. Horie and J. Hildebrandt, Dynamic compliance, limit cycles, and static equilibria of excised cat lung, *J. Appl. Physiol.*, 1971, **31**, 423–430.
5 P. A. Valberg and J. D. Brain, Lung surface tension and air space dimensions from multiple pressure-volume curves, *J. Appl. Physiol.*, 1977, **43**, 730–738.
6 S. Schürch, J. Goerke and J. A. Clements, Direct determination of surface tension in the lung, *Proc. Natl. Acad. Sci. U. S. A.*, 1976, **73**, 4698–4702.
7 T. A. Wilson, Relations among recoil pressure, surface area, and surface tension in the lung, *J. Appl. Physiol.*, 1981, **50**, 921–930.
8 S. Schürch, Surface tension at low lung volumes: dependence on time and alveolar size, *Respir. Physiol.*, 1982, **48**, 339–355.
9 J. C. Smith and D. Stamenovic, Surface forces in lungs. I. Alveolar surface tension-lung volume relationships, *J. Appl. Physiol.*, 1986, **60**, 1341–1350.

10 S. Schürch, H. Bachofen, J. Goerke and F. Possmayer, A captive bubble method reproduces the in situ behavior of lung surfactant monolayers, *J. Appl. Physiol.*, 1989, **67**, 2389–2396.
11 A. M. Bilek, K. C. Dee and D. P. Gaver, Mechanisms of surface-tension-induced epithelial cell damage in a model of pulmonary airway reopening, *J. Appl. Physiol.*, 2003, **94**, 770–783.
12 S. S. Kay, A. M. Bilek, K. C. Dee and D. P. Gaver 3rd, Pressure gradient, not exposure duration, determines the extent of epithelial cell damage in a model of pulmonary airway reopening, *J. Appl. Physiol.*, 2004, **97**, 269–276.
13 B. Robertson, in Pathology and pathophysiology of neonatal surfactant deficiency (''respiratory distress syndrome,'' ''hyaline membrane disease''), *Pulmonary Surfactant*, ed. Robertson, B.; Van Golde, L. M. G.; Batenburg, J. J., Elsevier Science Publishers, Amsterdam, 1 edn, 1984, pp. 383–418.
14 B. Lachmann, B. Robertson and J. Vogel, In vivo lung lavage as an experimental model of the respiratory distress syndrome, *Acta Anaesthesiol. Scand.*, 1980, **24**, 231–236.
15 A. Ivankin, I. Kuzmenko and D. Gidalevitz, Cholesterol-phospholipid interactions: New insights from surface x-ray scattering data, *Phys. Rev. Lett.*, 2010, **104**, 108101.
16 F. R. Dayeen, B. A. Brandner, M. W. Martynowycz, K. Kucuk, M. J. Foody, W. Bu, S. B. Hall and D. Gidalevitz, Effects of cholesterol on the structure and collapse of DPPC monolayers, *Biophys. J.*, 2022, **121**, 3533–3541.
17 J. M. Crane, G. Putz and S. B. Hall, Persistence of phase coexistence in disaturated phosphatidylcholine monolayers at high surface pressures, *Biophys. J.*, 1999, **77**, 3134–3143.
18 Y. Y. Zuo, R. Chen, X. Wang, J. Yang, Z. Policova and A. W. Neumann, Phase Transitions in Dipalmitoylphosphatidylcholine Monolayers, *Langmuir*, 2016, **32**, 8501–8506.
19 J. A. Clements, Functions of the alveolar lining, *Am. Rev. Respir. Dis.*, 1977, **115**(6 part 2), 67–71.
20 D. F. Tierney and R. P. Johnson, Altered surface tension of lung extracts and lung mechanics, *J. Appl. Physiol.*, 1965, **20**, 1253–1260.
21 J. N. Hildebran, J. Goerke and J. A. Clements, Pulmonary surface film stability and composition, *J. Appl. Physiol.*, 1979, **47**, 604–611.
22 L. Gunasekara, S. Schürch, W. M. Schoel, K. Nag, Z. Leonenko, M. Haufs and M. Amrein, Pulmonary surfactant function is abolished by an elevated proportion of cholesterol, *BBA, Biochim. Biophys. Acta, Mol. Cell Biol. Lipids*, 2005, **1737**, 27–35.
23 R. H. Notter, S. A. Tabak, S. Holcomb and R. D. Mavis, Dynamic surface pressure relaxation effects in binary mixed films containing dipalmitoyl phosphatidylcholine, *J. Colloid Interface Sci.*, 1980, **74**, 370–377.
24 B. I. Halperin and D. R. Nelson, Theory of two-dimensional melting, *Phys. Rev. Lett.*, 1978, **41**, 121–124.
25 B. Borie, X-ray diffraction in crystals, imperfect crystals, and amorphous bodies, *J. Am. Chem. Soc.*, 1965, **87**, 140–141.
26 P. Tippmann-Krayer and H. Möhwald, Precise determination of tilt angles by X-ray diffraction and reflection with arachidic acid monolayers, *Langmuir*, 1991, **7**, 2303–2306.
27 I. T. McGovern; D. Norman and R. H. Williams, in Surface science with synchrotron radiation, *Handbook on Synchrotron Radiation*, ed. Marr, G. V., Elsevier, Amsterdam, 1987, Vol. 2, pp. 467–539.
28 Y. Dai, B. Lin, M. Meron, K. Kim, B. Leahy and O. G. Shpyrko, A comparative study of Langmuir surfactant films: Grazing incidence x-ray off-specular scattering vs. x-ray specular reflectivity, *J. Appl. Phys.*, 2011, **110**, 102213.
29 Y. Dai, B. Lin, M. Meron, K. Kim, B. Leahy, T. A. Witten and O. G. Shpyrko, Synchrotron X-ray studies of rapidly evolving morphology of self-assembled nanoparticle films under lateral compression, *Langmuir*, 2013, **29**, 14050–14056.
30 L. G. Parratt, Surface studies of solids by total reflection of x-rays, *Phys. Rev.*, 1954, **95**, 359–369.
31 R. D. Smith and J. C. Berg, The collapse of surfactant monolayers at the air-water interface, *J. Colloid Interface Sci.*, 1980, **74**, 273–286.
32 E. C. Smith, J. M. Crane, T. G. Laderas and S. B. Hall, Metastability of a supercompressed fluid monolayer, *Biophys. J.*, 2003, **85**, 3048–3057.
33 W. Yan, S. C. Biswas, T. G. Laderas and S. B. Hall, The melting of pulmonary surfactant monolayers, *J. Appl. Physiol.*, 2007, **102**, 1739–1745.
34 H. Khoojinian, J. P. Goodarzi and S. B. Hall, Optical factors in the rapid analysis of captive bubbles, *Langmuir*, 2012, **28**, 14081–14089.
35 Y. Y. Zuo, M. Ding, A. Bateni, M. Hoorfar and A. W. Neumann, Improvement of interfacial tension measurement using a captive bubble in conjunction with axisymmetric drop shape analysis (ADSA), *Colloids Surf., A*, 2004, **250**, 233–246.
36 W. M. Schoel, S. Schürch and J. Goerke, The captive bubble method for the evaluation of pulmonary surfactant: surface tension, area, and volume calculations, *Biochim. Biophys. Acta, Gen. Subj.*, 1994, **1200**, 281–290.
37 V. M. Kaganer, H. Möhwald and P. Dutta, Structure and phase transitions in Langmuir monolayers, *Rev. Mod. Phys.*, 1999, **71**, 779–819.
38 H. B. Callen, *Thermodynamics; an introduction to the physical theories of equilibrium thermostatics and irreversible thermodynamics. In 163-167*, Wiley, New York, 1960, p. 376.
39 C. M. Knobler, Langmuir monolayers and liquid crystals, *Mol. Cryst. Liq. Cryst. Sci. Technol., Sect. A*, 2001, **364**, 133–140.
40 S. Q. Choi, K. Kim, C. M. Fellows, K. D. Cao, B. Lin, K. Y. C. Lee, T. M. Squires and J. A. Zasadzinski, Influence of molecular coherence on surface viscosity, *Langmuir*, 2014, **30**, 8829–8838.
41 K. Kjaer, J. Als-Nielsen, C. A. Helm, L. A. Laxhuber and H. Möhwald, Erratum: Ordering in lipid Monolayers studied by synchrotron X-Ray diffraction and fluorescence microscopy (*Physical Review Letters* 1987) **59**, 6 (744)), *Phys. Rev. Lett.*, 1987, **59**, 744.
42 K. Kjaer, J. Als-Nielsen, C. A. Helm, L. A. Laxhuber and H. Möhwald, Ordering in lipid monolayers studied by synchrotron x-ray diffraction and fluorescence microscopy, *Phys. Rev. Lett.*, 1987, **58**, 2224–2227.

43 C. A. Helm, H. Mohwald, K. Kjaer and N. J. Als, Phospholipid monolayers between fluid and solid states, *Biophys. J.*, 1987, **52**, 381–390.
44 D. R. Nelson, M. Rubinstein and F. Spaepen, Order in two-dimensional binary random arrays, *Philos. Mag. A*, 1982, **46**, 105–126.
45 R. Zangi and S. A. Rice, Phase transitions in a quasi-two-dimensional system, *Phys. Rev. E: Stat. Phys., Plasmas, Fluids, Relat. Interdiscip. Top.*, 1998, **58**, 7529–7544.
46 B. M. Discher, W. R. Schief, V. Vogel and S. B. Hall, Phase separation in monolayers of pulmonary surfactant phospholipids at the air-water interface: composition and structure, *Biophys. J.*, 1999, 77, 2051–2061.
47 B. M. Discher, K. M. Maloney, D. W. Grainger and S. B. Hall, Effect of neutral lipids on coexisting phases in monolayers of pulmonary surfactant, *Biophys. Chem.*, 2002, **101**, 333–345.
48 N. J. Gross, Pulmonary surfactant: unanswered questions, *Thorax*, 1995, **50**, 325–327.
49 S. Ardell, R. H. Pfister and R. Soll, Animal derived surfactant extract versus protein free synthetic surfactant for the prevention and treatment of respiratory distress syndrome, *Cochrane Database Syst. Rev.*, 2015, DOI: **10.1002/14651858.CD000144.pub2/abstract**.
50 W. Seeger, C. Grube, A. Gunther and R. Schmidt, Surfactant inhibition by plasma proteins: Differential sensitivity of various surfactant preparations, *Eur. Respir. J.*, 1993, **6**, 971–977.